Volume 1 | Number 1 | Jan 2013 | Pages 1–100

PCCP

Physical Chemistry Chemical Physics
www.rsc.org/pccp

ROYAL SOCIETY OF CHEMISTRY

ROYAL SOCIETY OF CHEMISTRY

www.rsc.org/pccp

Physical Chemistry Chemical Physics

ARTICLE

Locating the Nucleation Sites for Protein Encapsulated Gold Nanoclusters: A Molecular Dynamics and Fluorescence Study

B. A. Russell,[a] K. Kubiak-Ossowska,[b] P. A. Mulheran,[b] D. S. J. Birch[a] and Y. Chen[a†]

Fluorescent gold nanoclusters encapsulated by proteins have attracted considerable attention in recent years for their unique properties as new fluorescence probes for biological sensing and imaging. However, fundamental questions, such as the nucleation sites of gold nanoclusters within proteins and the fluorescence mechanism remain unsolved. Here we present a study of the location of gold nanoclusters within Bovine Serum Albumin (BSA) combining both fully atomistic Molecular Dynamic (MD) simulations and fluorescence spectroscopic studies. The MD simulations show gold clusters growing close to a number of cysteine sites across all three domains of BSA, although just two major sites in domains IIB and IA were found to accommodate large clusters comprising more than 12 atoms. The dependence of the fluorescence on pH is found compatible with possible nucleation sites in domains IIB and IA. Furthermore, the energy transfer between tryptophan and gold nanoclusters reveals a separation of 29.7Å, further indicating that gold nanoclusters were most likely located in the major nucleation site in domain IIB. The disclosure of the precise location of the gold nanoclusters and their surrounding amino acid residues should help better understanding of their fluorescence mechanism and aid their optimization as fluorescent nanoprobes.

Introduction

Understanding the structure and function of a biomolecule and its interactions with other molecules is very important to the advancement of many fields including medicine, pharmacy and biological sciences. Fluorescence spectroscopy and microscopy provide a strong set of tools to probe biomolecules by collecting the radiative information of a fluorophore, whether it is intrinsic or extrinsically attached to a biomolecule of interest. Fluorescent gold nanoclusters (NC) encapsulated by biomolecules have been demonstrated as a promising new type of fluorescent nanoprobe and have attracted considerable attention in recent years for their unique properties for biological sensing and imaging. [1-4] Due to their small size (~1nm, comparable to the Fermi wavelength of electrons) gold NCs have discrete electronic energy levels and size dependent fluorescence properties that also can be modified by surface chemistry.[5,6] This optical tunability, combined with their biocompatibility and photo stability, makes these fluorescence gold NCs surpass conventional dyes in many biomedical applications.

To date, a number of biomolecules have been successfully used to stabilize gold nanoclusters, such as Pepsin, Proline, Transferrin, Lysozyme, Human Serum Albumin (HSA) and Bovine Serum Albumin (BSA). [7-11] Among them, BSA encapsulated gold NCs (BSA-AuNC) have drawn considerable interest and demonstrable applications as biological sensors.[12,13] BSA has also shown great flexibility as a carrier of other molecules.[14] BSA is comprised of 3 domains, each of which can be separated into 2 subdomains.[15] Under acidic or basic conditions the 3 domains undergo well known conformational changes resulting in differences in the protein's micro-environments. Despite their great potential, the nucleation of gold NCs within the protein is unclear. Previous studies using X-ray photoelectron spectroscopy (XPS)[16] confirmed the existence of sulphur–gold bonds so that the gold clusters were believed to be near cysteine. However, there are 35 cysteine residues in BSA dispersed throughout the protein, and the exact location of the gold clusters within the protein cannot be discerned from just this fact. In contrast to atomically precise thiolate-protected gold nanoclusters, the uncertainty of the gold cluster location within protein hinders the understanding of the fluorescence mechanism (the paths in which the excited electron decay to the ground state) and the intelligent manipulation of the BSA-AuNC complex to improve their fluorescence characteristics.[17-20] Here we used both Molecular Dynamic simulations and fluorescence based experimental techniques to probe the nucleation of gold NCs within BSA. BSA in its normal form takes on the characteristic heart shape in a pH range of 4.3-8.0.[21] Using a MD model of the BSA protein and sequentially introducing gold atoms to the system, we tracked the growth of clusters within the BSA surface regions and discovered the possible nucleation sites. Further

[a.] Department of Physics, Strathclyde University, John Anderson Building, 107 Rottenrow, Glasgow G4 0NG, UK
[b.] Department of Chemical and Process Engineering, Strathclyde University, Glasgow G1 1XJ, UK
† corresponding author, email: y.chen@strath.ac.uk

experimental study, on the fluorescence characteristics at different pH and Förster Resonance Energy Transfer (FRET) between Tryptophan and gold nanocluster, narrows down the number of possible binding sites for gold NCs within BSA & HSA.

Methods

BSA-AuNC synthesis

BSA-AuNC was prepared following a one pot synthesis method.[11] Briefly, 51mg of $HAuCl_4$ was dissolved in 15ml of water at 37°C and 750mg of BSA was dissolved separately in 15ml of water at 37°C. The two solutions were then mixed together and stirred for 2 minutes. 0.5ml of 1.0M NaOH was pipetted into the mixture to bring the pH of the solution to >10. The solution was stirred for 6 hours at 37°C. The BSA-Au solution was transferred to a brown glass bottle and stored in an oven at 37°C for 48 hours. Buffer solutions were made at pH 1, 7 & 12 for the dialysis of BSA-Au nanoclusters. The BSA-AuNC was dialyzed in buffer solution for 24 hours and repeated three times. Finally BSA-Au solutions were diluted to 10% concentration using pure water before any measurements.

Fluorescence measurement and data analysis

Fluorescence emission/excitation spectra were measured using a Fluorolog 3 (Horiba). Time-resolved fluorescence measurements were performed using the time-correlated single-photon counting (TCSPC) technique on an IBH Fluorocube fluorescence lifetime system (Horiba Jobin Yvon IBH Ltd., Glasgow, UK) equipped with emission monochromator. Pulsed light sources (482nm Delta diode, 295nm Spectra-LED, 377nm Spectra-LED, 471nm Spectra-LED) operating at 1 MHz (for the diode based system) and 2kHz (for the LED based systems) repetition rates were used as excitation sources. Data analysis was performed using nonlinear least squares with the IBH iterative reconvolution software (DAS6 data analysis package). Multi-channel Scaling was used to measure decay associated spectra of BSA-AuNC over longer time scales. In order to find the lifetimes associated with the decay associated spectra a global fit method was applied to the sum of all the datasets measured. The lifetimes gained from the fitting were then used as fixed variables across each individual data set in order to calculate the relative intensities of each lifetime found at each emission wavelength measured. The standard deviations associated with the calculated lifetimes were obtained from fitting to the parabola that defines the minimum in the chi-squared goodness of fit parameter.

The standard deviations associated with the calculated lifetimes were obtained from fitting to the parabola that defines the minimum in the chi-squared goodness of fit parameter.

The Förster distance for Tryptophan and gold was calculated using the following equation:

$$R_0 = 0.211(k^2 n^{-4} Q_D J)^{1/6} \quad (1)$$

Where k^2 is the relative orientation of the transition dipoles of the donor and acceptor molecules, n is the refractive index of the medium, Q_D is the quantum yield of the donor in the absence of the acceptor molecule and J is the overlap integral describing the overlap of the donor emission and acceptor absorption. The Förster distance is related to the energy transfer via the following equation:

$$E = \frac{1}{1+(\frac{r}{Ro})^6} = 1 - (\frac{\tau}{\tau_0}) \quad (2)$$

Where r is the donor-acceptor separation, E is the efficiency of the energy transfer, τ is the lifetime of the donor in the presence of the acceptor and τ_0 is the lifetime of the donor in the absence of the acceptor.

Theoretical modeling

Using a Molecular Dynamics model of the BSA protein, single gold atoms were introduced to protein in the simulation. The BSA protein model (3V03) was downloaded from the Protein Data Bank [22] and the CHARMM27 [23] force-field was used with NAMD.[24] To emulate the conditions found in the one pot method used to synthesize BSA-Au [11] the protein was solvated in a rectangular box of water of size 116Å x 89Å x 101Å, and neutralized by adding NaCl at an ionic strength 0.05M, yielding over 93,000 atoms in the system. The simulation settings reproduced the conditions under pH 7. The protein was initially equilibrated for 300 ps at constant temperature of 300 K. Production simulations started by adding 25 gold atoms to the system with the protein. The simulation was pursued in the NVT ensemble for 100ns, following which another 25 gold atoms were added and the protocol was repeated until the total simulation length of 600 ns was obtained. The final structure consisted 150 gold atoms. For electrostatic interaction the PME method was used.[25] The above protocol was applied to BSA with and without disulphide bonds for the simulation time.

The gold potential proposed by Heinz et al. [26] (with Lennard-Jones parameters ε=-5.29; ½R_{min}=1.4755) was used for the gold atoms. Although there is current debate about the gold potential model (for example see the discussion in ref 27), we believe these parameters provide a useful and simple model with which we can explore the growth of gold clusters within accessible protein surface regions. We note that the interactions involving the gold atoms are described using Van der Waals parameters only, and favour hydrophobic interactions with the protein. In this study we make no attempt to model covalent bonding between gold and sulphur, since this type of interaction is beyond the scope of the empirical potential models used here. Nevertheless, we will be interested in the proximity of the gold clusters to the protein cysteine groups, since this will indicate the possibility of sulphur-gold bonding.

Using VMD[28] software the simulation allowed us to track the growth of clusters at various sites within BSA and also to measure the distances between different residues making up the protein structure. Molecular modelling of BSA-Au complexes was carried out using NAMD 2.8 software on the ARCHIE-WeSt supercomputer. Analysis of the modelling was carried out using VMD on ARCHIE-WeSt's visualization cores.

Results and discussion

MD simulation of Possible Gold Nanocluster Binding Sites Within BSA

Our initial study was to simulate the growth of BSA encapsulated gold nanoclusters. It was found that the initial uptake of the gold atoms to the protein was very fast with the majority of protein surface–gold atom interactions taking place within 1 ns of the addition of gold atoms. In the case with disulphur bonds broken, the uptake of gold atoms was found to be even quicker due to the increased flexibility of the protein. Initial protein surface interactions were found to take place predominantly at hydrophobic pockets formed by lysine and glutamic acid as seen in figure 1b) and to a lesser extent cysteine due to the residues proximity to the hydrophobic regions. When the disulphur bonds were broken, the propensity for the gold to cluster close to cysteine residues was seen to increase. After the 600 ns trajectories, both simulations showed that gold NCs nucleate close to cysteine sites, as shown by figure 2. The high affinity of gold to sulphur, as found in previous XPS studies,[11,16] suggests that this is reasonable result and that subsequent bonding between the gold and sulphur could occur (but is not modeled in this work as explained above). The gold atoms however were well dispersed in cluster sizes of 3-13
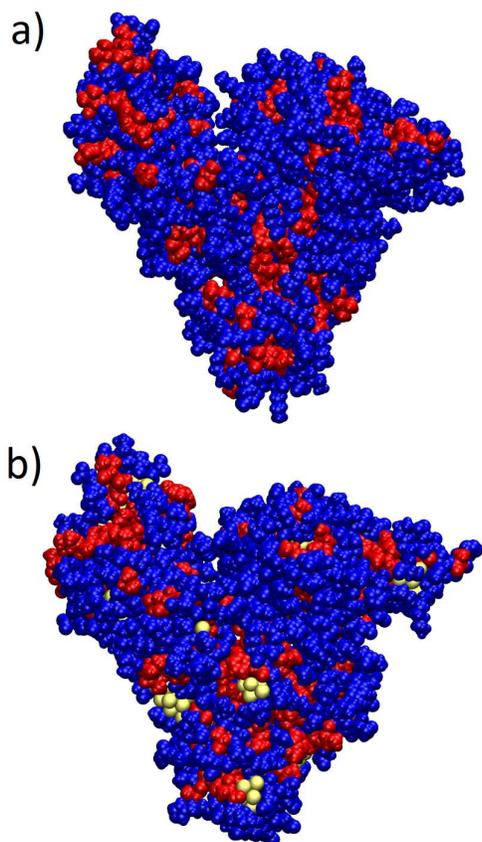

Figure 1. Hydrophobicity map of the BSA protein surface; a) before gold is introduced, b) after gold has bonded to protein. Hydrophilic regions are represented by blue while hydrophobic regions are represented by red. Gold nanoclusters not fully buried under the surface (represented by yellow) can be seen binding to only hydrophobic regions.
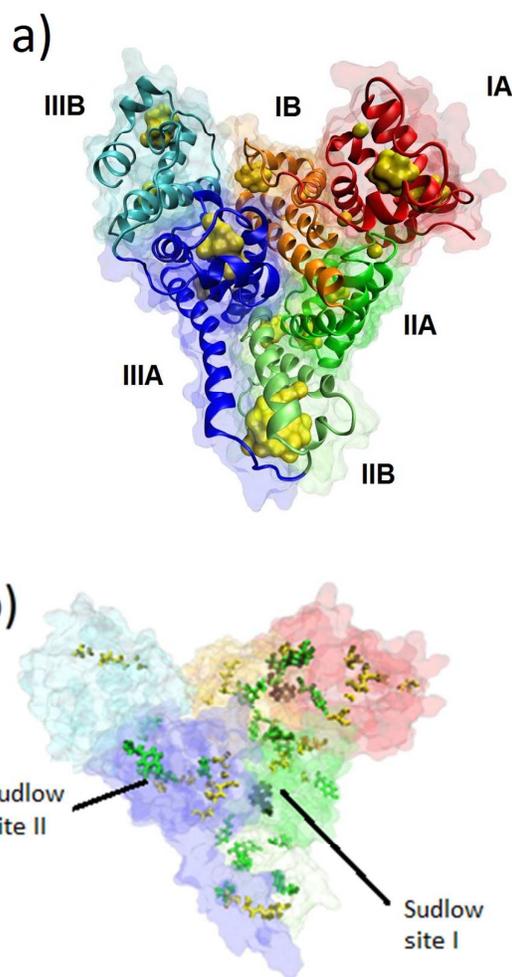

Figure 2. a) Molecular dynamic simulation of gold atoms nucleated within the protein after 600 ns of addition. Two large clusters can be seen in domains IA & IIB with smaller clusters dispersed throughout the protein. Gold clusters (yellow globules) can be seen to bond to sulphur atoms in cysteine residues. b) Cysteine residues can be seen in the same positions as the yellow globules in figure 1a) (represented by yellow chains). Tyrosine residues can be seen close to gold cluster location (represented by green chains). Tryptophan molecules are shown in domain IB and IIA (shown by black chains). Protein surface is shown as a ghost model in both cases, the colours indicate BSA subdomains: IA – red, IB – orange, IIA – green, IIB – light green, IIIA – blue, IIIB – cyan. The protein backbone is represented as a cartoon in a).

atoms around the protein, rather than nucleating in single particular site, as shown in figure 2a). Previous study on BSA-AuNC has found a cluster size around 25 atoms.[29] One possible reason for the smaller cluster sizes observed here could be the formation of multiple clusters. This is because gold atoms were introduced in random locations and gold atoms were seen to interact with many different parts of the protein surface and migrate to the nearest

cysteine residues, as seen in figure 2b). It is believed that tyrosine residues play a part in reducing gold salt in the one pot synthesis process; only 4 tyrosine residues are found on the BSA protein surface. Therefore in reality it might be possible that gold atoms only interact at certain areas of the protein surface and migrate to the nearest cysteine residues. Nevertheless, the simulation disclosed two major nucleation sites in IA and IIB, as shown in figure 2a). The nucleation site at IIB is of special interest as it close to the Sudlow binding site[14] which is located in a hydrophobic pocket in subdomain IIA [30], as shown in figure 2b). This is unsurprising as the proximity between sites and the ability for the Sudlow binding site (indicated in fig. 2a) to bind to many different molecules makes it a good candidate for the area where initial interaction with gold atoms takes place.

Fluorescence Spectroscopy Studies of BSA-Gold NCs at differing pH

In order to gain more insight on the gold nanocluster nucleation site/s within BSA the fluorescence properties of the gold nanocluster was studied. The red emission from BSA-AuNC and the long fluorescence lifetime associated with this emission was observed and attributed to the gold cluster rather than intrinsic fluorescence from the protein itself [8]. We thus focused on this red emission and studied how it was affected by the changes in the local environment of gold nanoclusters. pH dependent conformational changes of BSA have been well documented [19, 20, 31] and five conformational shapes of BSA observed. In extreme acidic conditions the protein undergoes a transition to what is known as the Extended form; with the transition taking place at pH lower than 2.7. In this form the alpha-helical structure of domain I become disrupted causing both domains I & II to unfold, resulting in the protein to unravel and become elongated. Prior to the protein becoming fully unfolded it takes on an intermediary form known as the Fast form at the pH range of 2.7-4.3. At this point the protein begins to unfold at domain III with a drop in alpha helix content. On increasing the pH to above 10 the protein takes on what is known as the Aged form. Here the secondary structure remains unchanged however alpha helices are known to become buried from solvent exposed positions.[32] Dynamic light scattering studies of BSA-AuNCs found hydrodynamic diameters of 24.9nm at pH1, 11.8nm at pH7 & 12.2nm at pH12, consistent with previous reports.[19,20,31]. The system was found to be monodisperse at pH7, but a small amount of larger particle sizes (>100nm, ~10% by volume) were seen at pH1 suggesting the formation of small amount of aggregators.

Figure 3 depicts the fluorescence emission spectra of BSA-AuNC at different pH excited at 295 nm. It is apparent that the fluorescence intensity is strongest when the protein is in its normal form. Upon increasing the pH to 12 the fluorescence intensity decreased by ~60%. This implies that while there are no changes to the protein secondary structure, the gold clusters' environment undergoes changes. Since the exposed alpha helices become buried in the Aged form, this suggests that the gold clusters are located in a part of the protein close to the surface. Lowering the pH of the sample to 1 caused a dramatic drop in fluorescence intensity (to 15 % of initial intensity). This indicates that the gold nanocluster is situated in either domain I or II, since the intensity drop is coincident with the unfolding of these domains. Moreover, decay associated spectra of the samples at differing pH were also measured using MCS over a 340 μs time range (2k repetition rate) in order to study the dependence of fluorescence lifetimes on pH. Three exponential fitting revealed two long fluorescence lifetime components and a

third short one (~ 1% of total intensity due to scattering effects) under 471 nm excitation.

Figure 4 compares the decay-associated spectra of BSA-AuNC at pH 1, 7 and 12. The corresponding decay associated spectral fluorescence lifetime data are listed in table S1-3 in supporting information. The long lifetimes at pH7, 2000±20 ns and 4730±40 ns, compare well with previously reported values.[33] At pH12 the lifetimes decreases significantly to 1170±30 ns and 2400±30 ns. There is also a change in the overall contribution of each lifetime with the longer lifetime contributing more to the overall fluorescence. At highly basic pH alpha helices located on the surface of the protein are known to become buried inside the protein.[9] If the gold nanocluster nucleation site is near one of these surface alpha helices, e.g., the nucleation site in IIB and IA, then at high pH the burying of helices could affect the hydrophobicity of the sites' micro-environment which could explain the decrease in fluorescence lifetime. At pH 1 the fluorescence lifetimes of the gold NCs were 1940±80 ns and 4460±90 ns. These lifetimes are nearly identical to the lifetimes found at pH 7, suggesting that the fluorescence originated from a similar system, i.e., a small number of gold NCs remain unaffected by the decrease in pH, possibly because some BSA remains in its normal form. While the lifetimes do not change upon lowering pH, the total intensity of the two long life-time components is seen to decrease by a factor of ~8, as shown in figure 4. This agrees well with the drop in fluorescence intensity found in figure 3.
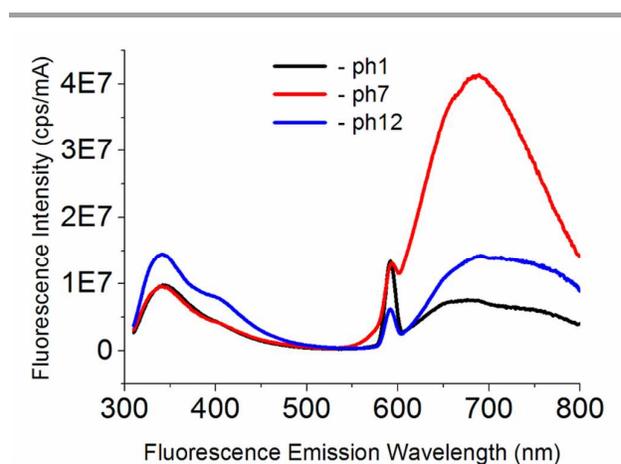

Figure 3. Fluorescence emission spectra of BSA-AuNC at pH 1(black), pH7 (red) and pH12 (blue), excited at 290nm.

The diminishing of both long lifetime components along with the total intensity can be explained by the unfolding of a majority of the protein molecules under strong acidic conditions, where fluorescence is quenched due to breaking of the sulphur-gold bonds and exposure of gold NCs to the surrounding solvent. Therefore, this again indicates that the fluorescent clusters are located at domain IA and IIB.
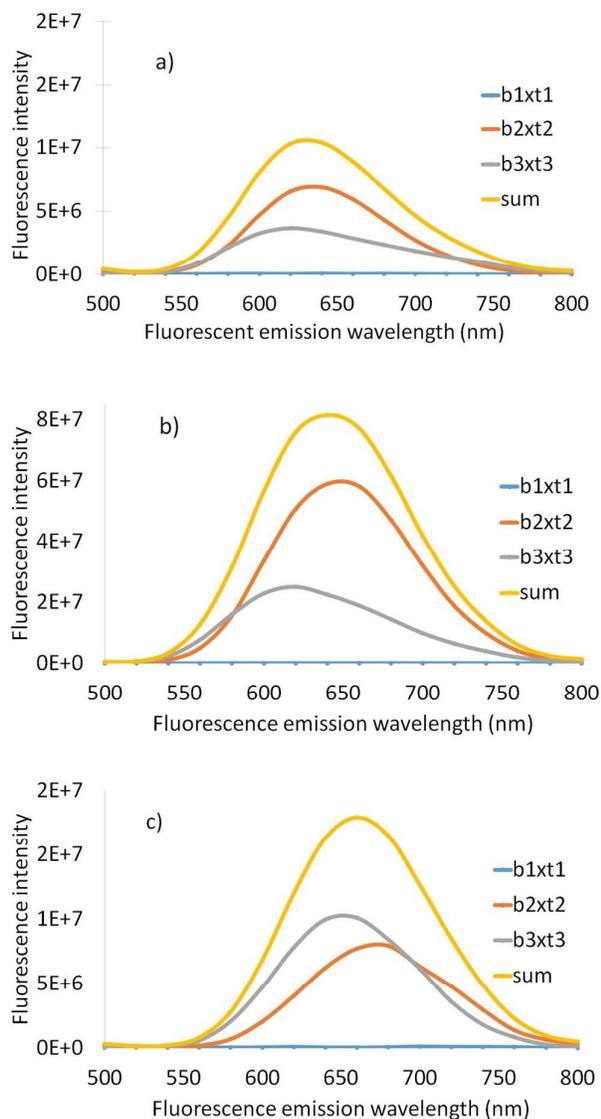
Figure 4. Decay associated spectra of BSA-AuNC at (a) pH 1; (b) pH 7; and (c) pH12. Three exponential fitting gave (a) t1 =220 ns, t2=1940 ns, t3=4460 ns; (b) t1=360 ns, t2=2000 ns, t3=4730 ns; (c) t1=190 ns, t2=1170 ns, t3=2400 ns.

Förster Resonance Energy Transfer between Tryptophan and Gold NCs in HSA-Gold

Förster resonance energy transfer, which occurs between donors and acceptors in close proximity, is referred to as the 'spectroscopic ruler' and has been employed to detect the separation between two molecular species. Here we studied the FRET between tryptophan and gold nanoclusters to further probe the location of gold NCs within BSA. Comparison of Tryptophan emission at 340 nm from BSA-AuNC and BSA alone showed a significant decrease in intensity when both were excited at 295 nm, figure 5. This together with the reduction in the fluorescence lifetime of tryptophan (not shown here), indicates the energy transfer between tryptophan and

gold nanoclusters, as reported previously.[34] Moreover, significant

increase of the emission from gold NCs at ~700 nm, as shown in figure 5, was observed under 295 nm excitation in comparison to those excited at 377 nm and 471 nm; about 16 times compared with UV and blue-greenish excitations. This suggests that energy transfer from tryptophan to gold NCs provides additional channels to the excitation of BSA-AuNC. As BSA contains two tryptophan residues, we used HSA to simplify the system because HSA contains a single tryptophan and both have similar structure. In order to find the separation distance, the fluorescence decay curves of tryptophan in HSA before and after gold nanocluster synthesis was measured (fig. S1-2 in supporting information). Multiple exponential lifetime fitting revealed an average lifetime of 4.33ns for tryptophan in HSA and 2.33 ns in HSA-AuNC. Förster distance and tryptophan - Au separation were found to be 30.14 Å and 29.74 Å, respectively, calculated using equations (1) and (2). Using the VMD software we were able to analyse the distances between the tryptophan residue and all cysteine residues in HSA using a model from the protein databank (4K2C).[35] The distance from the cysteine residues 316, 360, 361 and 369 (located in the major nucleation site in domain IIB) to tryptophan, as shown in figure 6, were found to be 28.79±3.23 Å, 27.29±3.23 Å, 29.52±3.23Å and 30.90±3.23Å respectively, matching with that from FRET analysis. This group of cysteine could be a favourable nucleation site as it is close to a tyrosine on the protein surface. Tyrosine is believed to play an important part in the reduction of gold salt [1]. The synthesis method requires a high pH (~10.5) due to the pKa of the side chain of Tyrosine being 10.1 [36] and most likely the place where electron transfer can take place between albumin and gold salt. On the other hand, the distance from other possible candidates located in domain IA, cysteine 91 and 75, to tryptophan was 35.6Å and 36.0Å, too large in comparison to the calculated separation. Therefore, the fluorescent gold clusters are mostly likely located in domain IIB and surrounded by Cysteine 316, 360, 361 and 369.
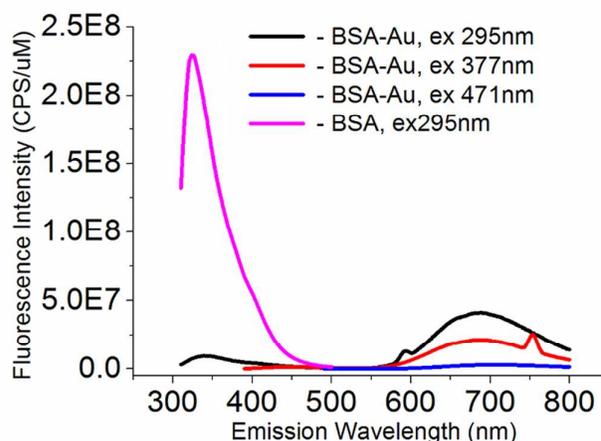

Figure 5. Fluorescence emission spectrum of BSA-AuNC excited at 295 nm (black), 377 nm (red) and 471 nm (blue) and BSA excited at 295nm (pink).

This result is significant as for the first time it reveals the precise location of the fluorescent cluster within a protein. This result

suggests that only a small number of cysteine residues are attached to the gold nanoparticle, although there are 35 of them in the protein. In fact, previous XPS measurement revealed a small number of Au(I) (~17%, 4 out of 25) present on the surface of the Au nanoparticle core.[11] This suggested a much smaller number of sulphur-gold bonds, compared to thiolate-protected gold nanoclusters, e.g., $Au_{22}SG_{18}$. Recently, Y. Bao, *et al.* has compared the fluorescent properties of gold NCs encapsulated using BSA and lysozyme.[37] Similar fluorescence lifetimes were found from these two systems despite the large difference in the total number of cysteine (35 vs. 8), again implying that only a few cysteine were involved in the fluorescent cluster formation. Because of the complexity of protein encapsulated gold nanoclusters, an explanation of the fluorescence mechanism is mainly based on the understanding of atomically precise thiolate-protected gold nanoclusters. The present work disclosed the precise location and surrounding residues of fluorescent gold nanoclusters, opening a new possibility of further unveiling the electronic structure of BSA-AuNC and fluorescence mechanism, and in turn manipulating the fluorescence process.
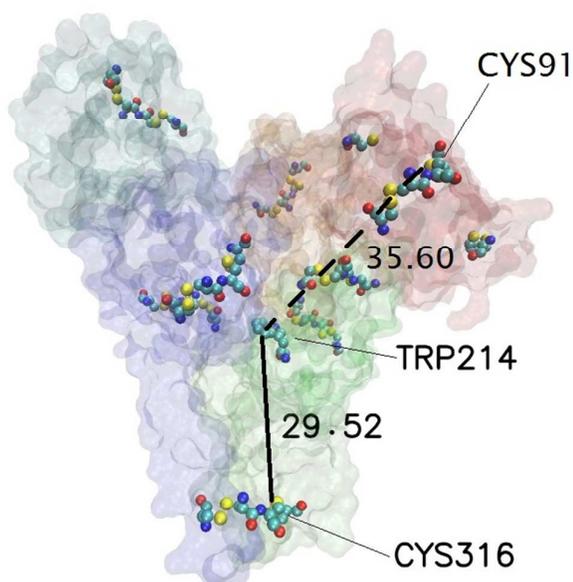

Figure 6. HSA protein model. The separation between tryptophan 214 and cysteine 316, indicated by a black solid line, was found to be 29.52 Å. The separation between CYS91 at domain IA and tryptophan 214, indicated by a dashed line, was found to be 35.60 Å. The protein colouring scheme used is the same as in Fig.1.

Conclusions

The location of gold NCs within Bovine Serum Albumin was investigated using both Molecular Dynamic simulations and fluorescence spectroscopy. The simulation showed that gold NCs have a strong tendency to bind to hydrophobic pockets on the protein surface, which traps them close to cysteine residues for subsequent chemical interaction. This agrees with a previous report on the nature of gold binding to BSA. Gold clusters were found to grow close to a number of cysteine

sites within all three domains of BSA, although two major growth sites, which accommodate large clusters of size >12 atoms, were identified in domains IA and IIB. By altering the pH of BSA-Au in solution, and studying the ensuing changes to the fluorescent properties, we have proposed that the gold atoms are nucleated in either domain I or II. Using Förster resonant energy transfer analysis we have found the separation of the gold nanocluster and tryptophan residue in HSA-Au to be 29.74Å. This separation matches the separation between tryptophan residue 214 and cysteine residue 316, both located in domain IIB, at 29.52Å. Fluorescent gold nanoclusters have unique optical properties quite different to the plasmonc effect normally associated with larger gold nanoparticles and have great potential in biomedical imaging and sensing.[38-46] Understanding the exact location of gold NCs within serum albumin is important to any future work to improve the fluorescent properties of these fluorophores; knowing the location will allow the alteration of the protein in ways whereby the fluorescent properties of the gold can be controlled.

Notes and references

1　L. Shang and G. U. Nienhaus, *Biophys. Rev*, 2012, **4**, 313-322
2　A. Retnakumari, S. Setua, D. Menon, P.Ravindran, H. Muhammed, T. Pradeep, S. Nair and M. Koyakutty, *Nanotechnology,* 2000, **21**, 055103
3　Z. Chen, G. Zhang, X. Chen, J. Chen, J. Liu and H. Yuan, *Biosens. Bioelectron*, 2013, **41**, 844-847
4　Y. Chen, W. Li, Y. Wang, X. Yang, J. Chen, Y. Jiang, C. Yu and Q. Lin, *J. Mater. Chem.* C, 2014, **2,** 4080
5　H. Kawasaki, K. Hamaguchi, I. Osaka and R. Arakawa, *Adv. Funct. Mater.* 2011, **21**, 3508–3515
6　D. E. Jiang, S. H. Overbury and S. Dai, *J. Am. Chem. Soc*. 2013, **135**, 8786–8789
7　A. R. Garcia, I. Rahn, S. Johnson, R. Patel, J. Guo, J. Orbulescu, M. Micic, J. D. Whyte, P. Blackwelder and R. M. Leblanc, *Colloids Surf. B. Biointerfaces*, 2013, **105**, 167–172.
8　X. Le Guevel, N. Daum and M. Schneider, *Nanotechnology*, 2011, **22**, 275103
9　X. Mu, L. Qi, P. Dong, J. Qiao, J. Hou, Z. Nie and H. Ma, *Biosens. Bioelectron*. 2013, **49**, 249–255
10　H. Wei, Z. Wang, L. Yang, S. Tian, C. Hou and Y. Lu, *Analyst,* 2013, **135**, 1406–10
11　J. Xie, Y. Zheng and J. Y. Ying, *J. Am. Chem. Soc*. 2009, **131**, 888–889
12　M. L. Cui, J. M. Liu, X. X. Wang, L. P. Lin, L. Jiao, L. H. Zhang, Z. Y. Zheng and S. Q. Lin, *Analyst*, 2012, **137**, 5346–5351
13　H. Lin, L. Li, C. Lei, X. Xu, Z. Nie, M. Guo, y. Huang and S. Bao, *. Bioelectron*. 2013, **41**, 256–261
14　K. Yamasaki, V. T. G. Chuang, T. Maruyama and M. Otagri, *Biochim. Biophys. Acta*. 2013, **1830**, 5435–5443

15 U. Anand and S. Mukherjee, *Biochim. Biophys. Acta*. 2013, **1830**, 5394–5404

16 X. Le Guevel, B. Hotzer, G. Jung, K. Hollemeyer, V. Trouillet and M. Schneider, *J. Phys. Chem. C*. 2011, **115**, 10955–10963

17 M. Zhu, C. M. Aikens, F. J. Hollander, G. C. Schatz and R. Jin, *J. Am. Chem. Soc.* 2008, **130**, 5883–5885

18 C. Zeng, H. Qian, T. Li, G. Li, N. L. Rosi, B. Yoon, R. N. Barnett, R. L. Whetten, U. Landman, R. Jin, *Angew. Chem. Int. Ed. Engl.*, 2012, **51**, 13114–13118

19 H. Qian, W. T. Eckenhoff, Y. Zhu, T. Pintauer, R. Jin, *J. Am. Chem. Soc.*, 2010, **132**, 8280–8281

20 P. D. Jadzinsky, G. Calero, C. J. Ackerson, D. A. Bushnell, R. D. Kornberg, *Science*, 2007, **318**, 430–433

21 M. Dockal, *J. Biol. Chem*., 2000, **275**, 3042–3050

22 K. A. Majorek, P. J. Porebski, A. Dayal, M. D. Zimmerman, K. Jablonska, A. J. Stewart, M. Chruszcz and W. Minor, *Mol. Immunol.* 2012, **52**, 174-182

23 N. Foloppe and J. A. D. Mackerell *Journal of Computational Chemistry*. 2013, **4**, 86-104

24 J. C. Philips, R. Braun, W. Wang, J. Gumbart, E. Tajkhorshid, E. Villa, C. Chipot, R. D. Skeel, L. Kale and K. Schulten, *J. Comput. Chem.* 2005, **26**, 1781–1802

25 U. Essmann, L. Perera, M. L. Berkowitz, T. Darden, H. Lee and L. A. Pedersen, *J. Chem. Phys.* 1995, **103**, 8577-8593

26 H. Heinz, R. A. Vaia, B. L Farmer and R.R. Naik, *J. Phys. Chem. C,* 2008, **112**, 17281-17290

27 K. Kubiak-Ossowska, P. A. Mulheran and W. Nowak, *J. Phys. Chem. B*, 2014, **118**, 9900–9908

28 W. Humphrey, A. Dalke and K. Schulten, *J. Mol. Graph.* 1996, **14**, 33–38

29 X. L. Cao, H. W. Li, Y. Yue and Y. Wu, *Vib. Spectrosc*. 2013, **65**, 186–192

30 O. K. Abou-Zied and N. Al-Lawatia, *Chem. Phys.chem*. 2011, **12**, 270–274

31 M. Bhattacharya, N. Jain, K. Bhasne, V. Kumari and S. Mukopadhyay, *J. Fluoresc*. 2011, **21**, 1083–1090

32 T. Peters and A. J. Stewart, *Biochim. Biophys. Acta*. 2013, **1830**, 5351–5353

33 S. Raut, R. Chib, S. Butler, J. Borejdo, Z. Gryczynski and I. Gryczynski, *Methods Appl. Fluoresc*. 2014*,* **2**, 035004

34 B. Mali, A. I. Dragan, J. Karolin and C. D. Geddes, *J. Phys. Chem. C*, 2013, **117**, 16650–16657

35 Y. Wang, H. Yu, X. Shi, Z. Luo, D. Lin, M. Huang, *J. Biol. Chem*., 2013, **288**, 15980-15987

36 N Taniguchi, J Baynes, M Dominiczak, *Medical Biochemistry,* 2010*,* **3**, 5-21

37 Y. Xu, J. Sherwood, Y. Qin, D. Crowley, M. Bonizzoni, Y. Bao, Nanoscale, 2014, **6**, 1515-1524

38 Y. Chen, Y. Zhang, D. J. S. Birch, A. S. Barnard, Nanoscale 2012, **4**, 5017.

39 Y. Zhang, J. Yu, D. J. S. Birch, Y. Chen, Proc. SPIE 2011, **7910** 79101H

40 Y. Zhang, D. J. S. Birch and Y. Chen, Appl. Phys. Lett. 2011, **99**, 103701

41 41 Y. Chen, J. A. Preece and R. E. Palmer, Ann. N. Y. Acad. Sci. 2008, **1130**, 201.

42 Y. Zhang, J. Yu, D. J. S. Birch, Y. Chen, J. Biomed. Opt. 2010, **15,** 020504-3.

43 P. Gu, D. J. S. Birch and Y. Chen, Methods Appl. Fluoresc. 2014, **2,** 024004.

44 C. Rachnor, M. R. Singh, Y. Zhang, D. J. S. Birch and Y. Chen, Methods Appl. Fluoresc. 2014, **2,** 015002.

45 Y. Zhang, G. Wei, J. Yu, D. J. S. Birch and Y. Chen, Faraday Discussion 178, 2014, 383-394.

46 C. Li, J. U. Sutter, D. J. S. Birch and Y. Chen, Nanotechnology, (IEEE-NANO) 2012.

Physical Chemistry Chemical Physics Accepted Manuscript